

Application of Doppler Effect in Speed Measurement of Traffic Vehicles in Roundabouts

Kaiyi Gu

NAS-NTFLS Cambridge International Centre, Nantong, Jiangsu, China

Abstract: Objective: To verify whether the Doppler effect can accurately measure the speed of the roundabout section. Methodology: First-hand research, conduct experiments. The speed of the remote-control trolley is measured at different frequencies and different speeds and the error is recorded, and the feasibility and the method of reducing the error are explored. Second-hand research, consult information. Understand the background knowledge of each module in the study, such as the development history of the Doppler effect, current traffic conditions, and commonly used traffic speed measurement devices. Results: This finding suggests that velocity is a critical factor influencing measurement accuracy in this experimental setup, while source frequency appears to have no meaningful impact on error rates. Conclusion: The accuracy of this measurement was found to improve as mainly the velocity increase. As for the effect of detection frequency on measurement accuracy, no strong correlation has been found, and the authors plan to use it as part of future research.

Keywords: Doppler effect, Roundabouts, Traffic, Speed measurement

1. Introduction

In today's society, traffic management through traffic speed measurement has become a key link in urban planning and road safety. With the increasing number of road vehicles, understanding and regulating traffic speed has become crucial. This is mainly reflected in two aspects, traffic congestion and traffic accidents. In terms of traffic congestion, taking Shanghai as an example, the road congestion has increased significantly in the first quarter of 2025. The number of congested road sections has increased from 36 in to 38. The average daily cumulative congestion time increased by 0.8 hours over the previous quarter, a year-on-year increase of 65.3 hours or 75.3% over last year (Command Center of Shanghai Municipal Transportation Commission, 2025). From the perspective of traffic accidents, the situation is equally challenging. According to (World Health Organization, 2024), the number of traffic deaths worldwide is about 1.19 million per year, with an average of more than 3,200 deaths due to car accidents every day.

In the 19th century, Christian Doppler first discovered and explained the phenomenon of the Doppler Effect (Guo & Sheng, 1993), which describes how the frequency of sound or light waves shifts because of relative motion between the source and the observer (Sang et al., 2014). Today, the Doppler effect has far exceeded its theoretical origins and gradually become an indispensable tool in modern transportation systems. Because of its great potential in real-world applications, Doppler Effect has been adapted to various transportation regulation systems where safety, efficiency, and innovation are intertwined.

Intersection crashes account for more than 45 percent of all crashes (US Department Of Transportation Federal Highway Administration, 2006). Although roundabouts was designed to alleviate this problem, (US Department of Transportation Federal Highway Administration, 2010) showed a 60-percent decrease in total crash rates, an 82-percent reduction in injury crash rates, a 100-percent decrease in the fatal crash rate, and a 27-percent reduction in property-damage-only crash rates, the accident rate in roundabouts remains high and there is still a large room for improvement.

The demand for smooth and safe transportation continues to grow and this study aims to understand and optimize the roles of the Doppler Effect in traffic detection and regulation, contributing to safer travel practices, as well as verify the possibility of applying the Doppler effect to circular road sections. In this study, on-site studies were first conducted to understand the current situation and characteristics of roundabouts in urban areas, particularly focusing on their design and traffic flow dynamics. Then, a comprehensive literature review was conducted to understand roundabouts as well as the Doppler Effect. Finally, a series of experiments were conducted to verify if the Doppler Effect can be used in calculating the speed of cars in roundabouts. This study provided insights about the feasibility of applying Doppler-based speed measurement in roundabouts and the potential for reducing traffic accidents through improved speed regulation.

2. Literature Review

2.1 Doppler Effect

The Doppler Effect describes the phenomenon where the frequency of a wave received by an observer deviates from its original frequency due to relative motion between the wave source and the observer. It is one of the fundamental principles of wave propagation. Since Austrian physicist Christian Doppler first proposed it in the 19th century, this effect has been widely applied in traffic monitoring radar (Roy et al., 2011), ocean sonar (Zhang et al., 2023), medicine (Wells, 1989), and many other fields.

Doppler-based speed measurement technologies obtain the target's velocity by detecting frequency shifts. In practical applications, from police road-speed enforcement to airport ground-vehicle monitoring and ocean acoustic navigation, they are gaining significant traction because of their non-contact, high precision, and real-time nature.

A Doppler speedometer typically includes a fixed wave emitter and a wave receiving system. By measuring the observed frequency f_o of the reflected wave, the target's velocity v_s can be inferred using the following formula:

$$f_o = \frac{c \pm v_o}{c \mp v_s} \cdot f_s$$

where f_s is the transmitted frequency, c is the wave propagation speed, and v_o is the detector's velocity. The detector is stationary in most cases, so the formula simplifies to:

$$f_o = \frac{c}{c \mp v_s} \cdot f_s$$

In traffic monitoring and similar applications, microwave radar emits high-frequency beams and receives signals reflected by vehicles. Due to the Doppler effect, the frequency of the reflected signal shifts relative to the transmitted signal. This frequency shift creates a measurable beat frequency (the difference between the transmitted and reflected frequencies), which is then used to accurately calculate the vehicle's speed. These systems can be further enhanced with video recognition algorithms and micro-controllers to achieve real-time image capture and speed analysis.

2.2 Fourier Transform

In order to analyze the frequencies of various waves, the Fourier transform (FT) is an essential core tool. Taking sound waves as an example, their essence is waves generated by air vibrations, and the directly collected sound signals (such as voltage changes recorded by microphones) belong to the "time domain signal", and it is difficult to directly see the frequency components. The Fourier transform becomes the best helper, which can decompose this time-domain signal into a superposition of sine or cosine waves of different frequencies, and view the signal from frequency domain.

Fast Fourier Transform (FFT) is a highly efficient algorithm for Fourier transforms, significantly reducing computational effort through mathematical optimization. Short-time Fourier transform (STFT) is also an advanced algorithm based on the Fourier transform, which splits a long signal into short frames and then performs a fast Fourier transform on each frame (Hu, 2005). In simple terms, their function is to turn sound waveforms that change over time into a frequency spectrum distributed by frequency, allowing you to see the "frequency component" of the sound.

2.3 Common Speed Measurement Methods for Roundabouts

2.3.1 Fixed Speed Cameras

Currently, fixed speed cameras are the most widely used speed measurement in roundabouts. Such cameras estimate the speed by calculating the time it takes for a vehicle to pass through a very small detection area (De Pauw et al., 2014). (National Highway Traffic Safety Administration, 2016) showed that implementing a fixed camera enforcement program on a 6.5-mile section of an urban highway resulted in a 44% to 54% reduction in total target accidents, a 28% to 48% reduction in injury accidents, and a 46% to 56% reduction in property damage accidents alone within 9 months.

While fixed speed cameras have proven to be effective, it has several limitations. Firstly, they can only measure the vehicle's instantaneous speed, failing to reflect the vehicle's behavior throughout the detection area. For example, if a driver slows down when approaching the camera but immediately accelerates significantly after passing it, the camera cannot capture the speeding behavior. Secondly, fixed speed cameras process data in the form of images, so they might fail to work under weathers with low visibility, such as heavy rain or fog.

2.3.2 Interval Speed Measurement System

The interval speed measurement system measures the speed by calculating the average speed of a vehicle over a certain distance. In roundabouts, measuring devices are typically installed at both the entrance and exit to obtain the driving time (a time interval), then the average speed was calculated with the known distance and driving time (Montella et al., 2012).

While the interval speed measurement system can detect the average speed of the vehicle in roundabouts, they cannot detect instantaneous dangerous driving behaviors, such as sudden speeding. Moreover, roundabouts have multiple entrances and exits so the interval speed measurement system will fail if a vehicle takes detours.

2.4 Challenges in Roundabout Speed Measurement

The traffic flow in the straight road section is one-way linear, the speed is relatively stable, and there are few sudden direction changes. The traffic flow of roundabouts is in a circular radiation, with multiple dynamic links such as convergence, circling, and exit, the speed fluctuates greatly, and vehicles from different directions intersect here.

There are fewer conflict points in the straight road section, mainly concentrated in side impacts (lateral or longitudinal) at intersections or when changing lanes; There are more conflict points on the roundabout, such as intersecting with the roundabout when entering or leaving the roundabout, rear-end collisions, or mixed traffic collisions when pedestrians and non-motorized vehicles cross the roundabout. The severity of accidents on straight roads is often directly related to vehicle speed, while that in roundabouts is closely related to the angle of collision (Eboli et al., 2020).

All in all, the ring road section has complex conditions compared to the straight road section, and the speed measurement is also more difficult. It is necessary to focus more on roundabouts.

2.5 Current State of Research

Early doppler speedometers used narrowband pulse technology but had limited ranging accuracy and time resolution (Skolnik, 2008). With advances in signal-processing techniques, such as wide band pulses, phased arrays, and coded echo have been introduced, significantly improving speed measurement accuracy, signal-to-noise ratio, and operational range.

(Scheiner et al., 2020) leveraged doppler radar to detect and track hidden objects outside direct line of sight in real-world automotive settings. Their approach fused temporal Doppler velocity sequences to recognize occluded vehicles and pedestrians, expanding radar applications into safety-critical domains. (Voulgaris & Trowbridge, 1998) evaluated the Acoustic Doppler Velocimeter (ADV) in a laboratory flume against Laser Doppler Velocimetry. They found mean velocities and Reynolds stresses could be measured with errors under 1%, demonstrating the instrument's capability for high-resolution turbulence quantification. (Naidoo et al., 2024) proposed a low-cost Continuous Wave (CW) doppler radar system capable of detecting vehicles and estimating their speeds in real-time for under 100 USD. They demonstrated that such an accurate system can be widely deployed in urban areas at minimal cost.

Although extensive research has examined the engineering implementation of doppler speed measurement, covering different types of radar, signal processing, and error analysis. There lacks systematic experimental work for measuring speed on non-linear paths, such as roundabouts. On the one hand, existing studies mostly focus on fixed linear paths or uniform reflective surfaces; on the other hand, real-world factors like vehicle acceleration/deceleration, changing path curvature, and radar angle deviation complicate the accurate interpretation of echo frequency shifts. The literature largely targets environments such as highways, airport runways, or underwater settings, with a notable absence of practical designs for complex dynamic traffic scenarios like roundabouts, where curvature continually changes and radar measurement angles must be constantly adjusted.

This research built a simple, controllable circular experimental platform. Using acoustic doppler modules, echo signals were collected at various positions to validate the relationship between calculated speed and frequency shift, and to investigate the patterns of measurement error. By modeling a roundabout track with a miniaturized doppler speed-measurement setup, this study verified the feasibility of using doppler-based speed measurement in roundabouts.

3. Methodology

The study combined both primary and secondary research. The experiment aimed to verify the applicability of the doppler effect in curve paths such as roundabouts. The core goal of the experiment was to evaluate the feasibility and accuracy of measuring the speed of moving objects using acoustic doppler shifts. This research focused on experimentally validating this effect in a roundabout vehicle speed-measurement system and providing an experimental model.

The study employed a low-cost, reproducible experimental design that substitutes electromagnetic waves (commonly used in traffic radar systems) with acoustic waves while maintaining identical physical principles, enabling further laboratory validation. The system systematically explored two key variables: the velocity of moving objects in curved trajectories

and frequency shifts of their acoustic waves. An overview the experiment setup was demonstrated in Figure 1.

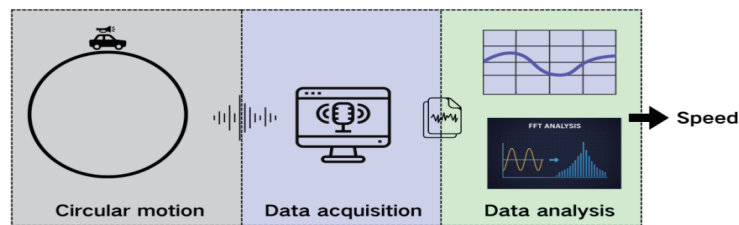


Figure 1: Overview of the system

3.1 Materials and Equipment

This experimental setup featured a cost-effective (less than 100 USD), modular design using consumer electronics. The motion system was a remote-controlled model car with a Bluetooth speaker mounted. The data acquisition system was made of a condenser microphone, which is capable of capturing at a sample rate of 44.1 kHz, and a computer with Audacity installed (Audacity, 2017). Data analysis and results visualization were performed with python. **NumPy** and **SciPy** were used to perform FFT/STFT, and **Seaborn** was used to visualize final results. The materials used in this study was summarized in Table 1 (VanderPlas, 2016).

Table 1: Materials used in the experiment

Category	Component	Description
Motion System	Remote-controlled model car	Drives the system with a Bluetooth speaker and three speed modes.
	Bluetooth speaker	Generates a 2–12 kHz pure-tone output.
	Rope and ruler	Fixes the car's circular path at a 50 cm radius.
Data Acquisition	Condenser microphone	Captures audio at a 44.1 kHz sampling rate from the edge of the circular path.
	Computer with Audacity installed	Records the audio and stores it as WAV files.
Data Analysis	Python (NumPy, SciPy, Matplotlib and Seaborn)	Analyzes the recorded data using FFT/STFT and visualizes the results.

3.2 Experimental Design and Setup

The remote-controlled model car was tethered to the center with a rope and it could only move along a circular path of 50cm radius. A Bluetooth speaker was mounted on the model car and it emitted a constant pure-tone sound. A condenser microphone was positioned at two radial distances to capture the sound signal, sampling at 44.1 kHz. Three speed settings (slow, medium, fast) were tested and the actual movement speed was verified via video analysis.

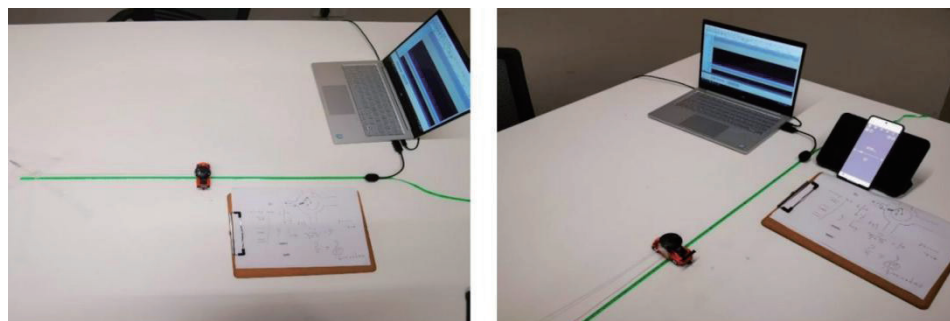


Figure 2: The experiment setup, Circular Motion (left) and Data Acquisition (right)

The experiments were conducted at five frequency levels: 2000, 4000, 6000, 8000, and 12000Hz, with all other conditions held constant. Each set of experiments lasted about 20 seconds, with the carts moving in circles at different speeds. The audio was recorded and saved as WAV files by Audacity. The sound wave's velocity is slow compared with electromagnetic waves, but doppler shifts can still be observed, making it suitable for indoor presentations. This method can reproduce the

principle of radar velocity measurement with sound waves.

3.3 Signal Processing and Velocity Calculation

The recorded audio signals were processed using FFT to extract the maximum frequency shift, which corresponds to the tangent point where the model car moves directly toward/away from the microphone.

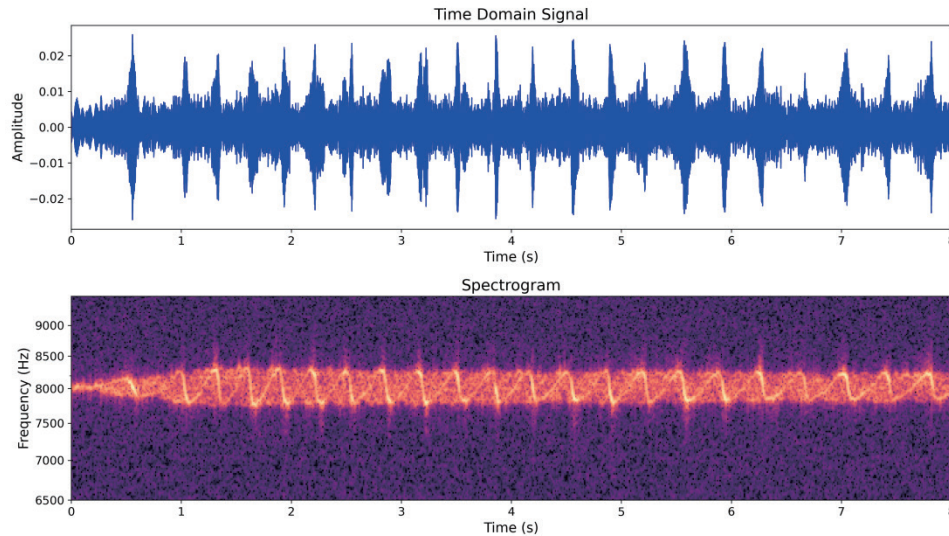


Figure 3: Spectrogram of the received signal (8000Hz)

This peak frequency f' was substituted into the Doppler equation:

$$v_s = v \left(\frac{f'}{f_0} - 1 \right)$$

where $v = 343 \text{ m/s}$ (the speed of sound) and f_0 is the source frequency. For ground-truth validation, the actual velocity was derived from video recordings by measuring the rotation period T and v_{actual} was obtained using the following formula:

$$v_{actual} = \frac{2\pi r}{T}$$

where $r = 50 \text{ cm}$. The absolute error and percentage error were then calculated to evaluate the method's accuracy.

4. Results and Visualization

4.1 Data collection

The following table was designed to record experiment data.

Table 2: Data collection table

Source $f(\text{Hz})$	Theoretical $v(\text{m/s})$	Theoretical peak $f(\text{Hz})$	Measured peak $f(\text{Hz})$	Calculated $v(\text{m/s})$	Absolute error	Percentage error
-----------------------	-----------------------------	---------------------------------	------------------------------	----------------------------	----------------	------------------

Source $f(\text{Hz})$ was the source frequency of the pure-tone sound emitted by the Bluetooth speaker. Theoretical peak $f(\text{Hz})$ was the theoretical peak frequency of the pure-tone sound. The maximum peak frequency was achieved at the tangent position when the model car moves toward the condenser microphone. Measured peak $f(\text{Hz})$ was the measured peak frequency and the data was obtained from Audacity. FFT and STFT were used to extract the peak frequency.

Theoretical $v(\text{m/s})$ was the actual approaching velocity of the model car, calculated with the formula for v_{actual} . Cal-

culated $v(m/s)$ was the estimated approaching velocity using the Doppler equation. The measured peak frequency was substituted into the Doppler equation to calculate the approaching velocity.

The absolute error is the difference between the actual approaching velocity and the estimated approaching velocity, and percentage error was absolute error divided by the actual approaching velocity.

To ensure robust and statistically significant results, the experiment was repeated multiple times under each experiment setup. For each of five frequency levels (2000 Hz , 4000 Hz , 6000 Hz , 8000 Hz , and 12000 Hz), nine separate trials were conducted, consisting of three repetitions at each of three speed levels (slow, medium, and fast). The collected raw data can be found in the Raw Data section of Appendix.

4.2 Results

4.2.1 Descriptive statistics

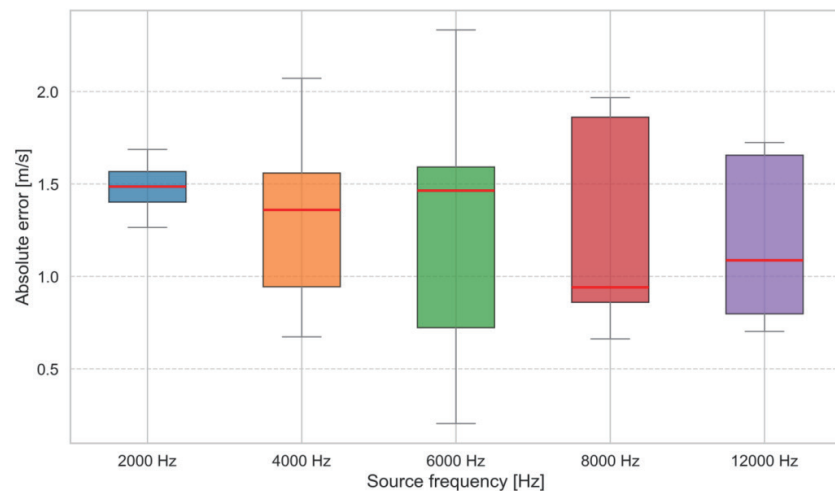


Figure 4: Absolute Error of different source frequency

The box plot shows the minimum, lower quartile, median, upper quartile and maximum value of the absolute error corresponding to the five groups of frequencies from 2000 to 12000 Hz. Taking the median of each group as the research object (the position of the red line segment), the wave source frequency changed from small to large, and the absolute error generally showed a downward trend, from 1.5 meters per second corresponding to 2000Hz to 1.2 meters per second corresponding to 12000Hz. Although the data in the middle group fluctuated a little, it was generally in line with expectations.

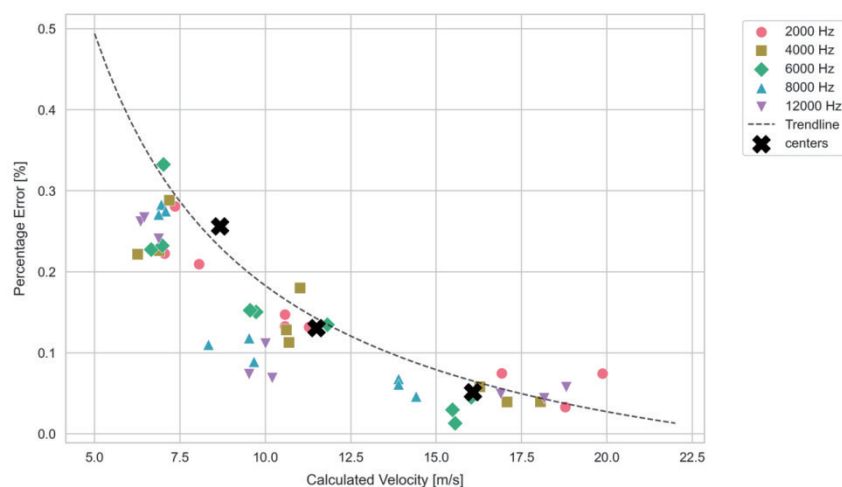


Figure 5: Percentage error of different velocity

From the above five sets of data of 2000-12000HZ, some patterns can be found. The percentage error demonstrated a correlation with both the speed of the object and the frequency of the wave source. Charts were made to analyze the relationship between object velocity and percentage error, source frequency and percentage error.

The spots of different shapes in the figure represent the velocity data of different groups from 2000HZ to 12000 HZ and the corresponding percentage errors. A fitting curve was drawn as the dotted line in Figure 5. The K-means algorithm is a clustering algorithm that first selects the K value and selects the initial center, and then repeatedly divides the data points to the nearest cluster, updating the cluster center until the center stabilizes or the iteration ends (Gan et al., 2020). From the K-means result (K=3), it was concluded these points corresponding to different data are obviously gathered in three areas, representing three motion states: slow, medium and fast. Specifically, slow speed corresponded to a speed of about 7 meters per second, with a percentage error of about 0.3%. The medium speed corresponded to a speed of about 10 meters per second, with a percentage error of about 0.15%; The fast speed corresponded to a speed of about 17 meters per second (the data in this range was more discrete because the car reached its horsepower limit and was difficult to control), with a percentage error of about 0.05%. It was concluded that the larger the original velocity of the object, the smaller the measured velocity error, so the error can be reduced by increasing the rotation speed of the object.

4.2.2 Inferential statistics

The Spearman correlation coefficient, calculated as

$$\rho = 1 - \frac{6 \sum d_i^2}{n(n^2 - 1)}$$

where d_i represents the rank differences and n is the sample size, confirms the absence of a monotonic relationship between source frequency and measurement error.

A highly significant strong negative correlation was identified between calculated velocity and percentage error (Spearman's $\rho = -0.823$, $p < 0.001$). This demonstrates that as velocity increases, the percentage error decreases substantially, supporting the visual pattern observed in Figure 5, where data points cluster into distinct regions corresponding to slow, medium, and fast motion states. The Spearman correlation analysis, which measures monotonic relationships without assuming linearity or normal distribution, reveals that approximately 67.7% (Coefficient of Determination = ρ^2) of the variance in percentage error can be explained by its relationship with velocity.

Based on the statistical analysis, the relationship between source frequency and percentage error was found to be statistically non-significant (Spearman's $\rho = -0.058$, $p = 0.705$), indicating that variations in source frequency do not systematically affect measurement accuracy. Although higher frequencies (8000Hz and 12000Hz) showed reduced error and discreteness due to better temporal resolution, the overall correlation across all frequency groups remains negligible (Ali Abd Al-Hameed, 2022).

This finding suggests that velocity is a critical factor influencing measurement accuracy in this experimental setup, while source frequency appears to have no meaningful impact on error rates. The strong negative correlation indicates that higher rotational speeds of the object yield more accurate results, providing a practical method for reducing measurement error. These results align with the box plot observations showing general downward trends in absolute error with increasing frequency. In practical speed measurement applications, supervisors are primarily concerned with whether high-speed vehicles are exceeding speed limits. The experimental results demonstrate that measurement errors are smaller at higher velocities, which means that speed measurement devices can effectively determine whether high-speed vehicles are speeding. This finding has significant practical implications for traffic monitoring and enforcement systems, as it indicates that the measurement accuracy improves precisely in the velocity range where accurate speed detection is most critical for safety and regulatory purposes.

5. Discussion

The current experimental design has several limitations, primarily due to the use of relatively low-level equipment. The speaker's frequency response was capped at 12kHz, with distortion occurring beyond this bandwidth, while the microphone's limited sensitivity fell short of professional standards. Additionally, the remote-controlled car's manual operation made it difficult to maintain a perfectly circular path, and its low maximum speed further restricted the experimental range. These equipment-related issues could be addressed by upgrading to higher-quality speakers and microphones when resources permit. For improved motion control, replacing the RC car with a stepper motor (Athani, 1997) would allow precise adjustments to rotation radius and speed, significantly enhancing the system's capabilities. In terms of the experimental environment, echo is not taken into account when measuring, which will result in echo interference during data analysis,

which can be carefully judged by humans.

From a theoretical perspective, $\Delta f = 2f \frac{v}{c}$, the frequency shift's visibility can be enhanced by either increasing the object's speed or using higher detection frequencies, as the shift magnitude is proportional to the product of these two variables. However, in practice, it may be due to the way FFT calculates the frequency and the final impact of the object's motion speed, and it may also be that our data is not enough to fully reflect the correlation. Nonetheless, the insights gained from this study provide a foundation for refining experimental setups and methodologies in future work.

6. Evaluation

6.1 Primary research

In conclusion, the speed accuracy of the car is the highest in the high-speed motion and the state of 12000 Hz. From the perspective of percentage error, the error of slow, medium and fast speeds is less than 0.4%, and the speed data obtained is relatively accurate. This error is even smaller if electromagnetic waves (such as radar) with a frequency much higher than sound waves are used in reality and faster speeds of real cars. Therefore, this experimental result can prove the theoretical feasibility of the calculation method as a whole.

6.2 Highlights

The raw experimental data were processed using FFT (Fast Fourier Transform) and STFT (short-time Fourier transform) in Python to extract meaningful frequency information. These signal processing techniques enabled precise calculation of key parameters, with results systematically summarized in Excel tables for further analysis.

For data visualization, Python's matplotlib and seaborn libraries were employed. While matplotlib served as the foundational plotting tool, seaborn enhanced the visual appeal of the charts. This combination ensured both efficiency and aesthetic quality, improving the clarity and professionalism of the presented results.

During the experiment, a novel approach was developed to determine object speed by analyzing periodic frequency changes in the sound signal. By measuring the time interval between consecutive crests in the frequency-time plot (STFT output) and combining this with the known rotation radius, the speed could be derived without relying on video recordings. This method is uniquely suited to circular motion studies, as linear motion lacks such periodicity.

While this frequency-based speed calculation proved efficient for controlled experiments, its application to real-world traffic monitoring (e.g., roundabouts) is limited. Vehicles in roundabouts rarely complete full circles, making the periodic signal analysis impractical. Nevertheless, the method remains valuable for idealized experimental setups, significantly reducing time and complexity compared to video-based techniques.

The use of Python for data processing and visualization greatly enhanced experimental efficiency. Automated analysis pipelines replaced manual calculations, ensuring comprehensive and accurate result presentation while minimizing human error. This computational approach underscores the growing importance of programming in modern experimental physics.

6.3 Secondary research

In the process of searching for literature resources, the authors tried to follow the principles of CRAAP. The first is currency (the timeliness of information). The author mainly collected information after 2010. The second point was the importance of the information, the author uses "roundabout" and "Doppler effect" as keywords when collecting data, and then screens useful information, so the final literature was in line with the needs. Then there was the authority (the source of the information) and accuracy (the reliability, truthfulness and correctness of the content) The information collected was from authoritative websites, literature and books. For example, the traffic data cited came from the Federal Highway Administration of the U.S. Department of Transportation, which was the official national agency of the U.S. government. It is authoritative and its data came from the statutory monitoring system, and its authenticity and accuracy were trustworthy.

7. Conclusion

Based on the experiment result, it was concluded that the Doppler effect can be used to accurately measure the speed of moving vehicles on circular path, such as roundabouts. The accuracy of this measurement was found to improve as mainly the velocity increase. As for the effect of detection frequency on measurement accuracy, no strong correlation has been found, and the authors plan to use it as part of future research. The authors hope that this study will provide some valuable information and ideas for traffic regulatory authorities and make a small contribution to strengthening traffic safety in the ring road section.

References

- [1] Ali Abd Al-Hameed, K. (2022). Spearman's correlation coefficient in statistical analysis. *International Journal of Non-linear Analysis and Applications*, 13(1), 3249-3255.
- [2] Audacity, T. (2017). Audacity. *The name audacity (R) is a registered trademark of dominic mazzoni* retrieved from <http://audacity.sourceforge.net>.
- [3] Command Center of Shanghai Municipal Transportation Commission. (2025). *The operation report of the Shanghai road network for the first quarter of 2025 has been released! The traffic volume of the road network has slightly increased compared to the same period last year*. Retrieved July 2nd from http://m.toutiao.com/group/7502378395540439592/?upstream_biz=doubao
- [4] De Pauw, E., Daniels, S., Brijs, T., Hermans, E., & Wets, G. (2014). An evaluation of the traffic safety effect of fixed speed cameras. *Safety science*, 62, 168-174.
- [5] Eboli, L., Forciniti, C., & Mazzulla, G. (2020). Factors influencing accident severity: an analysis by road accident type. *Transportation research procedia*, 47, 449-456.
- [6] Gan, G., Ma, C., & Wu, J. (2020). *Data clustering: theory, algorithms, and applications*. SIAM.
- [7] Guo, Y., & Sheng, H. (1993). *History of physics*. Tsinghua University Press.
- [8] Hu, G. (2005). *Digital Signal Processing: Theory, Algorithms and Implementation*. Tsinghua University Press.
- [9] Montella, A., Persaud, B., D'Apuzzo, M., & Imbriani, L. L. (2012). Safety evaluation of automated section speed enforcement system. *Transportation research record*, 2281(1), 16-25.
- [10] Naidoo, M., Paine, S., Mishra, A. K., & Gaffar, M. Y. A. (2024). Reliable Traffic Monitoring Using Low-Cost Doppler Radar Units. 2024 International Radar Conference (RADAR),
- [11] National Highway Traffic Safety Administration. (2016). *Speed Safety Camera Enforcement*. Retrieved July 29th from <https://www.nhtsa.dot.gov/book/countermeasures-that-work/speeding-and-speed-management/countermeasures/enforcement/speed-safety-camera-enforcement>
- [12] Roy, A., Gale, N., & Hong, L. (2011). Automated traffic surveillance using fusion of Doppler radar and video information. *Mathematical and Computer Modelling*, 54(1-2), 531-543.
- [13] Sang, D., Jones, G., Chadha, G., & Woodside, R. (2014). *Cambridge international as and a level physics coursebook with CD-ROM*. Cambridge University Press.
- [14] Scheiner, N., Kraus, F., Wei, F., Phan, B., Mannan, F., Appenrodt, N., Ritter, W., Dickmann, J., Dietmayer, K., & Sick, B. (2020). Seeing around street corners: Non-line-of-sight detection and tracking in-the-wild using doppler radar. Proceedings of the IEEE/CVF Conference on Computer Vision and Pattern Recognition,
- [15] Skolnik, M. I. (2008). Radar handbook. *IEEE Aerospace Electronic Systems Magazine*, 23(5), 41-41.
- [16] US Department Of Transportation Federal Highway Administration. (2006). *Task Analysis of Intersection Driving Scenarios: Information Processing Bottlenecks*. Retrieved eleventh August from <http://www.fhwa.dot.gov/publications/research/safety/06033/01.cfm>
- [17] US Department Of Transportation Federal Highway Administration. (2010). Retrieved eleventh August from <https://highways.fhwa.dot.gov/safety/learn-safety/noteworthy-practices/maryland-evaluates-safety-benefits-modern-roundabout>
- [18] VanderPlas, J. (2016). *Python data science handbook: Essential tools for working with data*. "O'Reilly Media, Inc."
- [19] Voulgaris, G., & Trowbridge, J. H. (1998). Evaluation of the acoustic Doppler velocimeter (ADV) for turbulence measurements. *Journal of atmospheric and oceanic technology*, 15(1), 272-289.
- [20] Wells, P. (1989). Doppler ultrasound in medical diagnosis. *The British journal of radiology*, 62(737), 399-420.
- [21] World Health Organization. (2024). *Despite notable progress, road safety remains urgent global issue*. Retrieved July 2nd from <https://www.who.int/news/item/13-12-2023-despite-notable-progress-road-safety-remains-urgent-global-issuea>
- [22] Zhang, S., Wu, J., & Yin, T. (2023). Simulation of sonar reverberation signal considering the ocean multipath and Doppler effect. *Frontiers in Marine Science*, 10, 1279693.

Appendix

Raw Data and Source Code						
Source $f(Hz)$	Theoretical $v(m/s)$	Theoretical peak $f(Hz)$	Measured peak $f(Hz)$	Calculated $v(m/s)$	Absolute error	Percentage error
2000	8.0554	2048.5344	2059.0000	9.7426	1.6872	20.95%
2000	7.3556	2044.2252	2057.0000	9.4215	2.0659	28.09%
2000	7.0487	2042.3405	2052.0000	8.6160	1.5673	22.24%
2000	10.5706	2064.1754	2073.0000	11.9730	1.4024	13.27%
2000	10.5742	2064.1977	2074.0000	12.1311	1.5570	14.72%
2000	11.2764	2068.6069	2078.0000	12.7623	1.4859	13.18%
2000	16.9176	2104.7260	2113.0000	18.1827	1.2651	7.48%
2000	18.7782	2116.9173	2121.0000	19.3965	0.6183	3.29%
2000	19.8709	2124.1432	2134.0000	21.3496	1.4787	7.44%
4000	6.8955	4082.8029	4102.0000	8.4544	1.5589	22.61%
4000	7.1890	4086.4034	4112.0000	9.2607	2.0717	28.82%
4000	6.2582	4075.0059	4092.0000	7.6442	1.3860	22.15%
4000	11.0154	4133.9321	4159.0000	12.9983	1.9829	18.00%
4000	10.6135	4128.8880	4146.0000	11.9730	1.3595	12.81%
4000	10.6893	4129.8388	4145.0000	11.8938	1.2045	11.27%
4000	18.0551	4224.3257	4233.7100	18.7687	0.7136	3.95%
4000	17.0739	4211.4895	4220.2800	17.7465	0.6726	3.94%
4000	16.2777	4201.1314	4213.4300	17.2226	0.9449	5.80%
6000	7.0125	6126.3558	6169.5700	9.3449	2.3324	33.26%
6000	6.6559	6119.8026	6147.7200	8.1697	1.5137	22.74%
6000	6.9813	6125.7824	6155.7600	8.6031	1.6217	23.23%
6000	11.8105	6215.9210	6246.2100	13.4020	1.5915	13.47%
6000	9.7263	6176.6951	6204.2100	11.1910	1.4647	15.06%
6000	9.5489	6173.3796	6200.7400	11.0070	1.4581	15.27%
6000	15.5524	6287.6108	6291.5800	15.7571	0.2047	1.32%
6000	15.4758	6286.1265	6295.1000	15.9384	0.4626	2.99%
6000	16.0285	6296.8508	6310.9400	16.7518	0.7233	4.51%
8000	6.9504	8166.9523	8215.4600	8.9169	1.9665	28.29%
8000	7.0757	8170.0244	8218.0500	9.0212	1.9456	27.50%
8000	6.8744	8165.0880	8210.9700	8.7358	1.8615	27.08%
8000	8.3331	8201.0002	8223.7100	9.2490	0.9159	10.99%
8000	9.5200	8230.4521	8258.5100	10.6428	1.1228	11.79%
8000	9.6664	8234.1013	8255.6000	10.5267	0.8602	8.90%
8000	13.9009	8341.0215	8365.1600	14.8418	0.9410	6.77%
8000	13.9009	8341.0215	8362.7800	14.7493	0.8485	6.10%
8000	14.4110	8354.0900	8371.1200	15.0733	0.6624	4.60%
12000	6.8744	12247.6321	12308.8300	8.5306	1.6563	24.09%
12000	6.3467	12228.2603	12289.5300	8.0101	1.6634	26.21%
12000	6.4509	12232.0825	12295.6200	8.1745	1.7236	26.72%
12000	10.2000	12371.1331	12397.5600	10.9030	0.7030	6.89%
12000	10.0051	12363.8264	12405.7500	11.1202	1.1152	11.15%
12000	9.5200	12345.6782	12372.0000	10.2231	0.7031	7.39%
12000	16.8903	12627.2897	12660.0000	17.7251	0.8348	4.94%
12000	18.1595	12677.0867	12708.5700	18.9568	0.7973	4.39%
12000	18.8119	12702.8380	12745.9600	19.8986	1.0866	5.78%

```

# Boxplot Style
colors = ['#1f77b4', '#ff7f0e', '#2ca02c', '#d62728', '#9467bd', '#8c564b']
for patch, color in zip(box['boxes'], colors[:len(frequencies)]):
    patch.set_facecolor(color)
    patch.set_alpha(0.7)

plt.setp(box['whiskers'], color='gray', linestyle='-')
plt.setp(box['caps'], color='gray')
plt.setp(box['medians'], color='red', linewidth=2)
plt.setp(box['means'], color='black', linestyle='--')

plt.xlabel('Source frequency [Hz]', fontsize=15)
plt.ylabel('Absolute error [m/s]', fontsize=15)
plt.grid(axis='y', linestyle='--', alpha=0.7)

plt.tight_layout()
plt.savefig('frequency_error_relationship.png', dpi=300, bbox_inches='tight')
plt.show()

# %%
frequencies = np.unique(np.array(data.iloc[:, 0]))

for i, f in enumerate(frequencies):
    v_theory = data.loc[data.iloc[:, 0] == f].iloc[:, 4]
    v_measure = data.loc[data.iloc[:, 0] == f].iloc[:, 7]

# Create figure
plt.figure(figsize=(10, 6))
plt.scatter(v_theory, v_measure, color='blue',
            label='Measured Data', alpha=0.7, s=80)

# Add y=x reference line (ideal case)
max_v = max(max(v_theory), max(v_measure)) * 1.05
plt.plot([0, max_v], [0, max_v], 'r--',
         label='Ideal Case (y=x)', linewidth=1.5)

```

```

# Formatting
plt.xlabel("Theoretical Velocity [m/s]", fontsize=12)
plt.ylabel("Measured Velocity [m/s]", fontsize=12)
plt.xlim(0, max_v)
plt.ylim(0, max_v)
plt.grid(True, linestyle='--', alpha=0.6)
plt.legend(fontsize=12, loc='upper left')
plt.savefig(f'veLOCITY_compare_{f}Hz_relationship.png', dpi=300, bbox_inches='tight')
plt.tight_layout()

# %%
# Set style for scientific plotting
sns.set(style="whitegrid", font_scale=1.2)
plt.figure(figsize=(12, 7))

# Create color mapping for different frequencies
frequency_groups = df["Source frequency [Hz]"].unique()
palette = sns.color_palette("husl", n_colors=len(frequency_groups))
color_map = dict(zip(frequency_groups, palette))

# Plot each frequency group with different markers
markers = ['o', 's', 'D', '^', 'v', 'p', '*']
for i, freq in enumerate(frequency_groups):
    subset = df[df["Source frequency [Hz]" == freq]
    plt.scatter(
        subset["Theoretical velocity [m/s]"],
        subset["Percentage error"],
        c=[color_map[freq]],
        s=120,
        marker=markers[i % len(markers)],
        label=f'{freq}',
        edgecolors='w',
        linewidth=0.5
    )

# Add trendline for overall pattern
z = np.polyfit(1.0/df["Calculated velocity [m/s]"], df["Percentage error"], 1)
p = np.poly1d(z)
plt.plot(np.linspace(5, 22, 50),
         p(1.0/np.linspace(5, 22, 50)),

```

```

        "k--", alpha=0.8, label='Trendline')

# Formatting
# plt.title("Velocity vs Percentage Error Across Frequencies", pad=20)
plt.xlabel("Calculated Velocity [m/s]", labelpad=10)
plt.ylabel("Percentage Error [%]", labelpad=10)
plt.legend(bbox_to_anchor=(1.05, 1), loc='upper left')

# Adjust layout
plt.tight_layout()
plt.savefig('velocity_error_relationship.png', dpi=300, bbox_inches='tight')
plt.show()

```